

Quantum interference between three two-spin states in a double quantum dot

S. A. Studenikin,¹ G. C. Aers,¹ G. Granger,¹ L. Gaudreau,^{1,2}
A. Kam,¹ P. Zawadzki,¹ Z. R. Wasilewski,¹ and A. S. Sachrajda^{1,*}

¹*Institute for Microstructural Sciences, National Research Council Canada, Ottawa, ON Canada K1A 0R6*

²*Département de physique, Université de Sherbrooke, Sherbrooke, QC Canada J1K 2R1*

Qubits based on the singlet (S) and the triplet (T_0 , T_+) states in double quantum dots have been demonstrated in separate experiments. It has been recently proposed theoretically that under certain conditions a quantum interference could occur from the interplay between these two qubit species. Here we report experiments and modeling which confirm these theoretical predictions and identify the conditions under which this interference occurs. Density matrix calculations show that the interference pattern manifests primarily via the occupation of the common singlet state. The S/T_0 qubit is found to have a much longer T_2^* as compared to the S/T_+ qubit.

Recently two semiconductor based qubits have been demonstrated individually in double quantum dots, based on a singlet and two different triplet states (S/T_0 and S/T_+) of two interacting spins. These qubits possess the advantageous property for qubit addressability in that quantum gate operations can be achieved by purely electrostatic means. The singlet and triplet states differ in their spin and, therefore, can interact (to form a qubit) due to the small statistical magnetic field gradients between the dots originating from the nuclear spins and the hyperfine interaction. As more complex quantum circuits and operations are developed [1–3] this raises the question whether and how these two qubits would interfere since they both include the singlet as a component state. In experiments to date this question has been purposely avoided by passing through the S/T_+ anticrossing fast enough to avoid involving the T_+ state [4] or by keeping far enough away from the S/T_0 interaction region.[5] However, in a recent theoretical paper on the coherent control of a two-electron spin system [6] Särkkä and Harju predicted that by using suitable pulses the two qubits should coexist resulting in a more complex pattern of coherent behavior with all three states involved. Here we present experimental and theoretical results confirming this prediction of an interplay between the singlet and triplet qubits in a double quantum dot.

For the experimental observation of the two kinds of singlet/triplet qubits we utilize a linear triple dot device [1–3] with gate voltages adjusted so that one of the dots acts as a "spectator" with exchange energy to the central dot close to zero in the detuning range of interest. Under these conditions the remaining two dots may be regarded as a double dot and the relevant states can be described in the language of singlet and triplet states [4, 5].

An SEM image of the device is shown in Fig. 1(a). For these experiments charge detection measurements are made with the quantum point contact (QPC) [8] on the left side of the device. The charge state of the device and tunneling between dots are controlled using a combination of gates 1 and 2, which are also connected to high frequency lines.

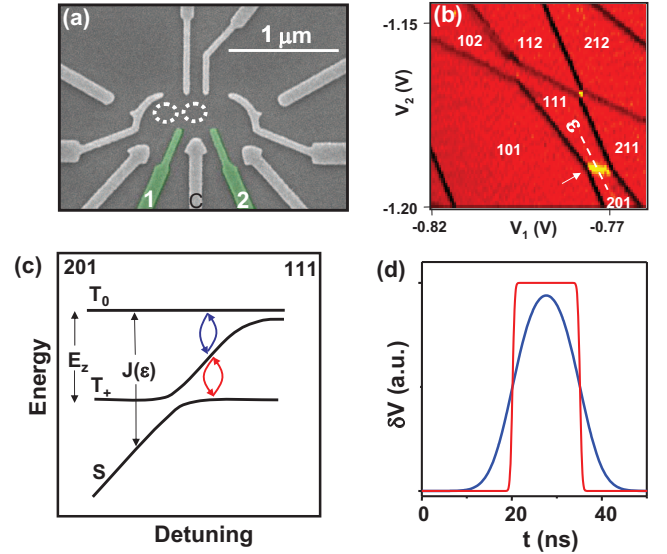


FIG. 1: (a) Electron micrograph of the triple dot device. Fast voltage pulses ($\delta V_1, \delta V_2$) are applied to gates 1 and 2 in addition to DC voltages (V_1, V_2). Gate C tunes the (1,1,1) region size and can be adjusted such that the pair of dots indicated by the white ovals operate independently of the right "spectator dot". (b) Stability diagram obtained from numerically differentiating the left QPC detector conductance with respect to V_2 at $B=0.2$ T. Black is low, red is medium, and yellow is high. Charge addition lines appear black, and charge transfer lines appear yellow [3]. A detuning line is drawn across the (2,0,1)/(1,1,1) charge transfer line indicated by the white arrow. (c) Schematic energy diagram of the two-spin states near the (2,0,1)/(1,1,1) charge transfer line. (d) Examples of the pulse shapes for a pulse duration $\tau=15$ ns after Gaussian filtering, leading to rise times of 8.0 (blue) and 0.8 ns (red).

The charge detection stability diagram obtained in the absence of pulses is shown in Fig. 1(b). We focus on coherent spin manipulation in a spin qubit regime between the $(N_L, N_C, N_R)=(1,1,1)$ and $(2,0,1)$ electronic charge configurations, or $(1,1)/(2,0)$ in the double dot notation. The C gate is tuned to make the (1,1,1) region wide enough (>15 mV along V_2) such that the right dot

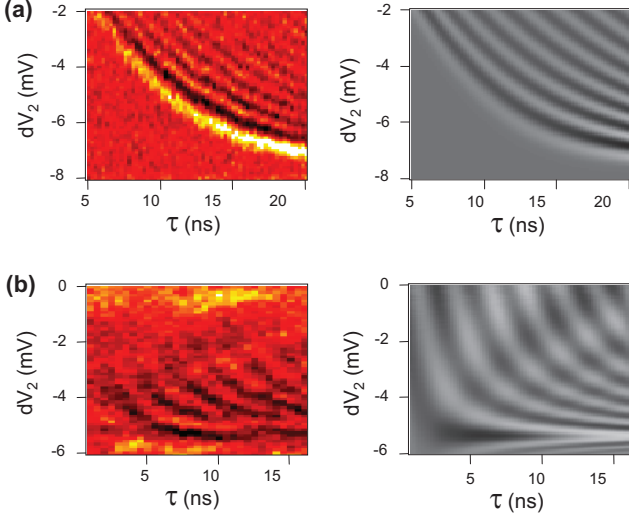


FIG. 2: (a,b) Left panels: experimental maps in the $\tau - V_2$ plane from the numerical derivative of the QPC conductance with respect to detuning component V_2 for the pulse rise times (a) 8.0 ns and (b) 0.8 ns. For (a) [(b)] the pulse involves $(\delta V_1, \delta V_2) = (-5, 10)$ mV [(-4, 8) mV] to traverse the charge transfer line between (2,0) and (1,1) and repeats every $T_m = 0.5 \mu s$, $B = 0.08$ T. Black is low, orange is medium, and yellow is high transconductance. Right panels: calculated derivative with respect to detuning of singlet probability P_S in the $\tau - V_2$ plane for the rise times of the left panels. Black (white) is low (high). dV_2 shift is due to 2 mV pulse change between (a) and (b).

contribution is negligible. The two dots acting as a double dot are indicated by the white ovals in Fig. 1(a). The white dashed line in Fig. 1(b) illustrates a detuning line ϵ whose V_2 component corresponds to the abscissa in Fig. 1(c). In the two dot language used in the remainder of this letter this detuning line crosses the (2,0)/(1,1) charge transfer line.

The lowest electronic states of a double dot containing two electrons consist of two singlet states, $S(2,0)$ and $S(1,1)$, and three triplet states, T_- , T_0 , and T_+ . The latter are split by the Zeeman energy in an applied in-plane magnetic field. The two singlet states anticross as a function of detuning due to charge coupling between the dots. By changing gate voltages to move along the detuning dashed line ϵ in Fig. 1(b) the ground state singlet S can be tuned to cross the $T_+(1,1)$ triplet state and approach the $T_0(1,1)$ state asymptotically as illustrated in Fig. 1(c). [4, 5, 7] The S and T_0 states are split by the exchange energy $J(\epsilon)$. The S and T_+ states cross at a detuning which depends upon magnetic field. Nuclear hyperfine field gradients between the dots cause the S/T_+ crossing to become an anticrossing and the S/T_0 spacing to be asymptotically nonzero. Here we plot the triplet states as horizontal lines as in [7] and restrict the diagram to only three relevant levels S , T_+ and T_0 .

The spin dynamics in response to a voltage pulse is cal-

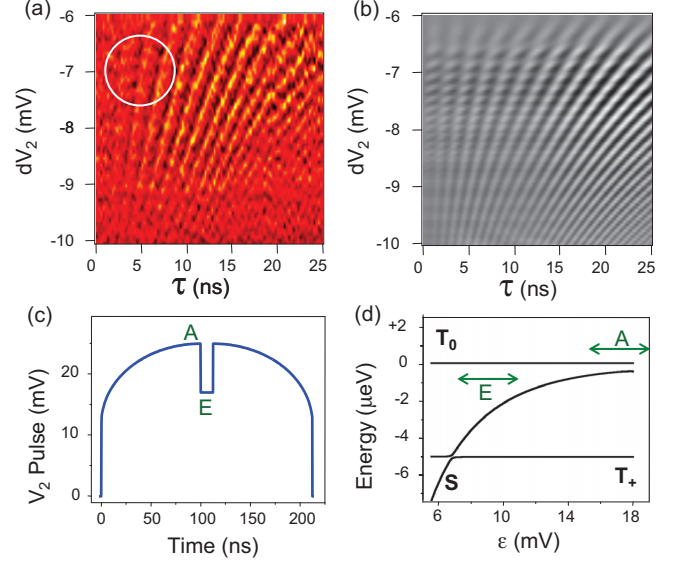


FIG. 3: (a): Experimental map in the $\tau - V_2$ plane from the numerical derivative of the QPC conductance with respect to detuning component V_2 for an elliptical pulse rise shown in (c), repetition time $T_m = 2 \mu s$, $B = 0.2$ T. Circle indicates region showing non-adiabatic structure on fringes. Black is low, orange is medium, and yellow is high transconductance. (b): Calculated derivative with respect to detuning of P_S in the $\tau - V_2$ plane. Black (white) is low (high). The origin for the pulse detuning is the charge transfer line. (c): Pulse shape added to the DC detuning. (d) Energy diagram, including hyperfine splitting, showing the detuning ranges of the adiabatic (A) and exchange (E) steps. The effective energy/gate voltage lever arm used here is $38.1 \mu eV/mV$.

culated from the time dependence of the density matrix ρ in the $S/T_+/T_0$ system with a Hamiltonian:

$$H = \begin{pmatrix} E_{T_0} & 0 & \Gamma_{S,T_0} \\ 0 & E_{T_+} & \Gamma_{S,T_+} \\ \Gamma_{S,T_0}^* & \Gamma_{S,T_+}^* & E_S \end{pmatrix} \quad (1)$$

where the energies on the diagonal are those in the absence of nuclear hyperfine interactions. These hyperfine terms appear as Γ_{S,T_+} and Γ_{S,T_0} which are respectively the differences between the dots of the (x,y) and z hyperfine fields [7]. In all the calculations shown here we take $\Gamma_{S,T_+} = \Gamma_{S,T_0} = 0.2 \mu eV$ (a typical value to fit the observed experimental fringe contrast[1]).

The time evolution of ρ is calculated from an initial state at large negative detuning where $P_S = 1$, using:

$$\frac{d\rho}{dt} = i[\rho, H/\hbar] \quad (2)$$

This yields a set of three differential equations solved numerically by the Runge-Kutta method.

Filtering a rectangular pulse controls the rise time [Fig. 1(d)]. At long (short) rise times, pulses appear

Gaussian (almost rectangular). Standard spin to charge conversion techniques are used in the region $S(2,0)$ during spin projection measurements to obtain the singlet occupation probability P_S [13]. Applying a detuning pulse of duration τ will result in a phase accumulation between the quantum state components. This phase is related to both the accumulation time and the detuning voltage. [1, 5, 6, 11, 12]

The dependence of the oscillations on rise time is shown in the left panels of Fig. 2(a,b) for a large enough detuning pulse to allow mixing with the S/T_0 states (the graphs in this letter use the pulse detuning dV_2 component defined with respect to the observed charge transfer line). For optimum observation of the S/T_+ oscillations a rise time of a few ns is usually required as shown in the left hand panel of Fig. 2(a). This is due to a competition between the Landau-Zener tunneling probability during the passage through the anticrossing and the restriction imposed by the coherence time. [1] The S/T_+ fringes have a negative slope in the τ - V_2 plane. However, if the rise time is shortened to less than 1 ns an interplay between the two qubit species becomes manifest. The S/T_+ oscillations weaken (as the Landau-Zener tunnelling probability approaches unity [9, 10]) and S/T_0 oscillations with a positive gradient appear across the S/T_+ oscillations [see left panel Fig. 2(b)]. The calculated results agree well with experimental data as shown in the right panels of Fig. 2(a,b). The opposite slopes for the two qubits occur because as a function of detuning the level spacing decreases in one qubit while increasing in the other (see Fig. 1(c)).

On varying the interdot coupling we find the contrast visibility of the S/T_0 fringes improves substantially. We speculate that this results from less sharp detuning dependence of the S/T_0 splitting and hence a lower sensitivity to charge noise effects. We therefore switch to a voltage configuration in which the conditions for the two dot approximation are still upheld but where the interdot coupling is stronger, in this case $61 \mu\text{eV}$ compared to $17 \mu\text{eV}$ for Fig. 2(a,b). Due to this larger coupling the applied magnetic field range is also larger in this regime and fields up to 1T may be used (in what follows we use $B = 0.2 \text{ T}$). In this regime more oscillations are visible and the interplay clearer. We first demonstrate the S/T_0 qubit alone. To achieve this we perform a variation of the "spin-swap" scheme [4] using a pulse, illustrated in Fig. 3(c), consisting of a fast 12 mV segment to cross the S/T_+ from the initial detuning dV_2 to $\epsilon = dV_2 + 12 \text{ mV}$ followed by a 100 ns adiabatic elliptical pulse to $dV_2 + 25 \text{ mV}$ in the S/T_0 interaction region (region A in Fig. 3(d)) and then a rapid step backwards to $dV_2 + 17 \text{ mV}$ (region E in Fig. 3(d)) where the finite exchange splitting causes rapid oscillations during a time τ . The pulse then follows the reverse path back to the initial detuning for spin to charge readout. The adiabatic step in this scheme rotates the state vector on the S/T_0 Bloch sphere down to

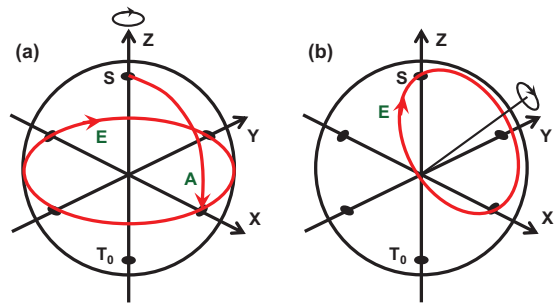


FIG. 4: (a): Schematic of S/T_0 Bloch sphere showing state vector motion corresponding to steps A and E of the "spin swap" pulse of Fig. 3(c). Ideally optimized axis of rotation during the exchange step E is around the Z-axis. (b): Schematic state vector motion corresponding to the "fast" square pulse of Fig. 1(d). Axis of rotation is lowered towards the equator.

the equator which maximizes the effect of exchange rotation (see Fig. 4(a)). The resulting fringes are shown in Fig. 3(a) to be compared to the calculation in Fig. 3(b). The internal structure of the fringes in theory and experiment (see circled region in Fig. 3(a)) is related to slight non-adiabaticity in the elliptical part of the pulse. We observe S/T_0 oscillations persisting to 25 ns in Fig. 3(a).

Having observed S/T_0 oscillations in the stronger coupling regime we return to a fast pulse scheme as in Fig. 1(d) to observe interactions between all 3 states. The experimental results in this regime are shown in Fig. 5(a) for a 1 ns pulse rise time. At large negative detuning over twenty S/T_+ coherent oscillations are seen.

At less negative detuning strong S/T_0 oscillations are seen without recourse to the initial adiabatic initialization step introduced in Ref.[4] to rotate the state vector to the equator on the Bloch sphere as illustrated in Fig. 4(a). We note, however, that our S/T_0 fringes are essentially the same as those observed in the adiabatic initialization scheme although the period is larger because the detuning range extends to regions of smaller splitting between S and T_0 . Such a pulse shape produces strong oscillations in the weak exchange interaction regime close to the S/T_0 asymptotic region where the axis of qubit rotation on the S/T_0 Bloch sphere is not purely around the Z axis but is tilted downwards towards the equator producing enhanced visibility (see Fig. 4(b)). At intermediate detunings we observe the regime where the two qubits coexist and qubit interplay is clearly visible. The T_2^* for the S/T_+ interaction in the theoretical calculation is 10 ns which is similar to values found in previous work on double [5] and triple dots [1]. Interestingly the S/T_0 fringes in the region where the energy splitting is small appear to persist to much longer times in contrast to a value of 10 ns quoted in [4] and in Fig. 5(b) we use an infinite T_2^* for S/T_0 . In fact, as illustrated in Fig. 5(c), we frequently see oscillations for pulse durations exceed-

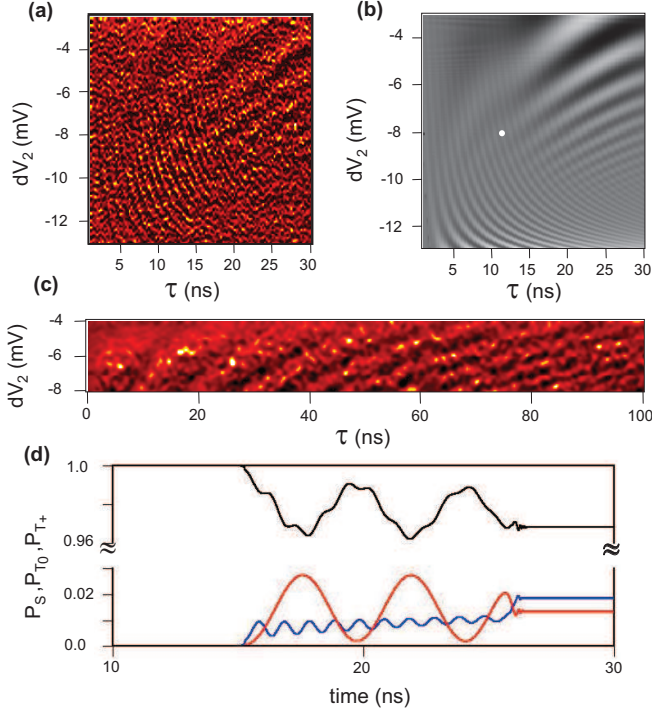


FIG. 5: (a): Experimental map in the $\tau - V_2$ plane from the numerical derivative of the QPC conductance with respect to detuning component V_2 for a pulse rise time of 1.0 ns. The pulse involves $(\delta V_1, \delta V_2) = (-16.2, 20.0)$ mV to traverse the charge transfer line between (2,0) and (1,1) and repeats every $T_m = 2 \mu s$, $B = 0.2$ T. Black is low, orange is medium, and yellow is high transconductance. (b): Calculated derivative with respect to detuning of P_S in the $\tau - V_2$ plane for the same rise time as in (a). Black (white) is low (high). The origin for the detuning voltage is the charge transfer line. (c): Narrow detuning region with rectangular pulse, $(\delta V_1, \delta V_2) = (-19.5, 25.0)$ mV, rise time ≈ 0.25 ns. (d): Time response of P_S (black), P_{T_0} (red) and P_{T_+} (blue) to single pulse at point on Fig. 5(b) indicated by white dot.

ing 100 ns when the rise time is very short. We find T_2^* is shorter for smaller detunings consistent with charge noise limiting an enhanced coherence time. It has been suggested that such an enhancement could originate either from non-zero exchange and/or an incidental narrowing of the nuclear environment [14, 15]. To see the detailed nature of the oscillations involving both S/ T_0 and S/ T_+ interactions we choose a point on the calculated map Fig. 5(b) indicated by the white dot and plot the time dependence of the state occupation probabilities P_S , P_{T_0} and P_{T_+} as a function of time before, during and after the pulse. This theoretical analysis of the quantum interference process finds the common component singlet state, S, is strongly affected by both qubit modulations while the two triplet states fundamentally retain their individual oscillatory character.

In conclusion we have studied a scenario where two

qubits, S/ T_0 and S/ T_+ , sharing a common component state, coexist and interplay. The main feature in this evolution of a three state system is a quantum interference effect. The relative strength of each qubit contribution can be tuned with the rise time of the pulse responsible for the quantum state preparation. Simulations provide good agreement with the experimental results. The T_0 and T_+ components show the individual oscillations for the appropriate interaction while the S component shows both. The S/ T_0 qubit, triggered by the perpendicular component of the statistical nuclear field gradient persists an order of magnitude longer than the S/ T_+ qubit driven by the in-plane component. This longer coherence time is consistent with a lower sensitivity to charge noise.

We acknowledge discussions with Bill Coish, Michel Pioro-Ladrière, Aash Clerk, Guy Austing and Roland Brunner, and O. Kodra for programming. A.S.S. acknowledges funding from NSERC and CIFAR. G.G. acknowledges funding from the NRC-CNRS collaboration.

* Electronic address: Andrew.Sachrajda@nrc.ca

- [1] L. Gaudreau, G. Granger, A. Kam, G. C. Aers, S. A. Studenikin, P. Zawadzki, M. Pioro-Ladrière, Z. R. Wasilewski, and A. S. Sachrajda, *Nature Phys.* DOI: 10.1038/NPHYS2149 (2011).
- [2] L. Gaudreau, A. Kam, G. Granger, S. A. Studenikin, P. Zawadzki, A. S. Sachrajda, *Appl. Phys. Lett.* **95**, 193101 (2009).
- [3] G. Granger, L. Gaudreau, A. Kam, M. Pioro-Ladrière, S. A. Studenikin, Z. R. Wasilewski, P. Zawadzki, and A. S. Sachrajda, *Phys. Rev. B* **82**, 075304 (2010).
- [4] J. R. Petta, A. C. Johnson, J. M. Taylor, E. A. Laird, A. Yacoby, M. D. Lukin, C. M. Marcus, M. P. Hanson, and A. C. Gossard, *Science* **309**, 2180 (2005).
- [5] J. R. Petta, H. Lu, and A. C. Gossard, *Science* **327**, 669 (2010).
- [6] J. Särkkä and A. Harju, *New J. of Phys.* **13**, 043010 (2011).
- [7] J. M. Taylor, J. R. Petta, A. C. Johnson, A. Yacoby, C. M. Marcus, and M. D. Lukin, *Phys. Rev. B* **76**, 035315 (2007).
- [8] M. Field, C. G. Smith, M. Pepper, D. A. Ritchie, J. E. F. Frost, G. A. C. Jones, and D. G. Hasko, *Phys. Rev. Lett.* **70**, 1311 (1993).
- [9] S. Shevchenko, S. Ashhab, and F. Nori, *Physics Reports* **492**, 1 (2010).
- [10] C. Zener, *Proc. R. Soc. Lond. A* **137**, 696 (1932).
- [11] H. Ribeiro and G. Burkard, *Phys. Rev. Lett.* **102**, 216802 (2009).
- [12] H. Ribeiro, J. R. Petta, and G. Burkard, *Phys. Rev. B* **82**, 115445 (2010).
- [13] K. Ono, D. G. Austing, Y. Tokura, and S. Tarucha, *Science* **297**, 1313 (2002).
- [14] W. A. Coish and D. Loss, *Phys. Rev. B* **72**, 125337 (2005).
- [15] W. A. Coish, *Nature Phys.* **5**, 710 (2009).